Alexandria Engineering Journal (2023) 75, 627–638

HOSTED BY

Alexandria University

Alexandria Engineering Journal

www.elsevier.com/locate/aej
www.sciencedirect.com

ORIGINAL ARTICLE

# Chaos in a two dimensional fractional discrete Hopfield neural network and its control

**Abdallah Al-Husban [a], Rabia Chaimaà Karoun [b,*], Ahmed Salem Heilat [c], Mohammed Al Horani [d], Amina Aicha Khennaoui [e], Giuseppe Grassi [f], Antonio Vincenzo Radogna [g], Adel Ouannas [h]**

[a] *Department of Mathematics, Irbid National University, 2600 Irbid, Jordan*
[b] *Department of Mathematics, The University of Jordan, 11942 Amman, Jordan*
[c] *Department of Mathematics, Jadara University, 2600 Irbid, Jordan*
[d] *Department of Mathematics, The University of Jordan, 11942 Amman, Jordan*
[e] *NTIC Faculty, University of Constantine 2, 25000 Constantine, Algeria*
[f] *Dipartimento Ingegneria Innovazione, Universita del Salento, 73100 Lecce, Italy*
[g] *Dipartimento Ingegneria Innovazione, Universita del Salento, 73100 Lecce, Italy*
[h] *Department of Mathematics, University of Oum El-Bouaghi, 04000 Oum El Bouaghi, Algeria*

Received 26 February 2023; revised 11 May 2023; accepted 21 May 2023
Available online 15 June 2023

**KEYWORDS**

Chaos;
Control;
Fractional discrete system;
Hopfield neural network

**2000 MSC**

0000;
1111

**Abstract** A novel two-dimensional fractional discrete Hopfield neural network is presented in this study, which is based on discrete fractional calculus. This network incorporates both constant and variable orders, and its behavior is examined using phase plots, time evolution, bifurcation, Lyapunov exponents, and complexity analysis. Compared to integer and constant fractional orders, the numerical simulations demonstrate that the proposed variable-order fractional HNN exhibits more complex characteristics, and by selecting different fractional variable orders, novel attractors with chaotic behavior can be obtained. Additionally, a control scheme is proposed to stabilize the suggested neural network by utilizing the stability theorem for fractional discrete time systems. This control scheme is applied to both states in the study.



## 1. Introduction

The theory of fractional calculus is old as its inception can be attributed to two of the most prominent figures of modern calculus, L'Hopital and Leibniz, as early as 1695. The complete framework for this type of calculus was complete by the 1800s. Traditionally the term fractional calculus has referred to studying integration and differentiation of noninteger order.

* Corresponding author at: The university of Jordan, departement of mathematics, Amman 11942, Jordan.
E-mail addresses: dralhosban@inu.edu.jo (A. Al-Husban), karoun.ch13@gmail.com (R.C. Karoun), heilat@jadara.edu.Jo (A.S. Heilat), horani@ju.edu.jo (M.A. Horani), amina.khennaoui@univ-constantine2.dz (A.A. Khennaoui), giuseppe.grassi@unisalento.it (G. Grassi), antonio.radogna@unisalento.it (A.V. Radogna), ouannas.adel@univ-oeb.dz (A. Ouannas).

Peer review under responsibility of Faculty of Engineering, Alexandria University.

https://doi.org/10.1016/j.aej.2023.05.078

Several definitions of fractional derivatives, including Riemann–Liouville, Caputo, Riesz–Caputo and Grunwald–Letnikov derivatives, are available in the literature. As a generalization of integer-order derivatives and integrals, fractional calculus considers non-integer orders, taking into account the model's history or "memory effect." This feature has rendered fractional calculus an important tool for describing biological and physical phenomena [1–4]. Moreover, significant advancements have been made in the stability, control, and synchronization of fractional systems [5–8].

The theory and application of neural networks have been widely explored in various domains, including associative memory, combinatorial optimization, pattern recognition, and signal processing.

As a result, neural networks are considered one of the most crucial nonlinear models in the field of nonlinear research. The significance of neural networks can be primarily attributed to their structure and ability to perform parallel processing.

Recently, artificial neural networks have gained significant attention among scientists working in fields associated with the human brain [9]. These networks are considered to be one of the most advanced technologies for deep learning and fall under the umbrella of artificial intelligence [10]. The first investigation of artificial neural networks dates back to 1943 when McCulloch and Pitts conducted research in this area. Since then, engineers and scientists have applied their findings to various electrical and engineering applications, including electrical circuit switching, picture and signal processing, machine learning, and power circuits[11].

As fractional calculus plays a crucial role in the formulation of various phenomena, neural networks were fictionalized and later referred to as fractional-order neural networks. This breakthrough has resulted in the publication of numerous research papers on the topics of chaos, control, stability, synchronization, and dynamic analysis of fractional-order neural networks in both continuous and discrete time. These advancements in the field of fractional-order neural networks have been documented in several papers and researches, including references [12–17].

Applying the results and methods used in the neural networks with fractional variable order is challenging due to the complex dynamics involved. As a result, there have been limited research papers published on the study of fractional variable-order neural networks, including [18–21]. It is worth noting that the fractional variable order is a special case of fractional order systems where the order of the equation is a continuous function between 0 and 1. By improving the complex dynamics of discrete-time HNN, it has the potential to provide a valuable approach in this field of research. This paper presents a significant contribution to the topic by introducing a novel two-dimensional variable fractional order discrete Hopfield neural network (DHNN). We achieved this by studying the discrete-time Hopfield neural network with a constant fractional order, which has not been previously presented in the literature. Then we utilize the Caputo-like difference operator on discrete Hopfield neural network system with fractional variable order, as introduced by Hopfield in integer form in [22]. This work led to the birth of Hopfield neural network systems, as documented in references [23–25]. By proposing this new DHNN model, we are providing a promising avenue for further research in this field. This paper is organized as follows: Section 2 is devoted to discuss different complex dynamics of a new two dimensional fractional discrete Hopfield neural network with constant order and an adaptive controller is proposed to establish the stability of the system state's. In Section 3, we investigate the dynamics of the proposed fractional Hopfield neural network with variable order through phase plots, bifurcation and maximum Lyapunov exponents. Section 4 consists of a summary and conclusions of the whole work.

## 2. A discrete Hopfield neural network with fractional constant orders

The Hopfield neural network (HNN) is a simplified biological nervous system that is often used to mimic the human brain. There are two types: discrete Hopfield neural networks (DHNN) and continuous Hopfield neural networks (CHNN) [22]. This work concentrate on the discrete HNN with fractional order. Its mathematical expression is given by:

$$\begin{aligned} {}^{C}\Delta_{\theta}^{\eta} y_k(s) &= -v_k y_k(s+\eta-1) + \sum_{l=1}^{n} E_{kl}\phi_l(y_l(s+\eta-1)) + X_k, \\ &\quad \forall s \in \mathbb{N}_{\theta+1-\eta}, \forall k = 1,2,\ldots,n, \end{aligned} \tag{1}$$

in which $\theta \in \mathbb{R}$ is the starting point and:

- $\phi_l : \mathbb{R} \to \mathbb{R}$ depicts the neuron activation function.
- $E = (E_{kl})_{n\times n}$ indicates the weights matrix that specifies the connection between neurons $k$ and $l$.
- $v_k > 0$ are the parameters of self-regulating neurons.
- $X_k$ are the external inputs.
- The fractional difference operator ${}^{C}\Delta_{\theta}^{\eta}$ is used in the sense of the $\eta$-Caputo-like difference operator which is defined as follows[26]:

$$\begin{aligned} {}^{C}\Delta_{\theta}^{\eta} g(s) &= \Delta_{\theta}^{-(j-\eta)} \Delta^{j} g(s) \\ &= \frac{1}{\Gamma(j-\eta)} \sum\nolimits_{k=\theta}^{s-(j-\eta)} \frac{\Gamma(s-k)}{\Gamma(s-k-j-\eta+1)} \Delta^{j} g(k), \end{aligned} \tag{2}$$

where $j = [\eta] + 1$, and $\eta \notin \mathbb{N}$. The main advantage of using the Caputo difference operator is that the initial condition does not need to be specified in order to solve an equation or a system of equations

As this paper mainly focuses on investigating the effect of fractional order on the dynamics of neural network, we consider a system with two neurons, for simplicity, the synaptic weight matrix $E$ is chosen as:

$$E = \begin{bmatrix} \beta & -\gamma \\ 1 & \beta \end{bmatrix}, \tag{3}$$

and $\phi_l(y_l) = \sin(y_l)$, $v_k = 1$, $X_k = 0$. As a result, we get the following fractional discrete HNN with two neurons:

$$\begin{cases} {}^{C}\Delta_{\theta}^{\eta} y_1(s) = -y_1(s+\eta-1) + \beta \sin(y_1(s+\eta-1)) \\ \qquad\qquad -\gamma \sin(y_2(s+\eta-1)), \\ {}^{C}\Delta_{\theta}^{\eta} y_2(s) = -y_2(s+\eta-1) + \sin(y_1(s+\eta-1)) \\ \qquad\qquad +\beta \sin(y_2(s+\eta-1)), \end{cases} \tag{4}$$

where $s \in \mathbb{N}_{\theta+1-\eta}$, $\mathbb{N}_{\theta} = \{\theta, \theta+1, \theta+2, \cdots\}$, $\theta \in \mathbb{R}$ is the starting point and $\eta \in (0,1]$ is the fractional order.

In order to discuss the complex dynamics of the proposed system, we shall present the theorem below, which will enable us to acquire the numerical formula for the DTHNN (4).

**Theorem 1.** [27] The solution of the **IVP**

$$\begin{cases} {}^{C}\Delta_{\theta}^{\eta} y(s) = f(s+\eta-1, y(s+\eta-1)) \\ \Delta^{m} y(\theta) = y_m, \quad k = \lceil \eta \rceil + 1, \quad m = 0, 1, \ldots, k-1, \end{cases} \tag{5}$$

is expressed as

$$y(s) = y_0(\theta) + \frac{1}{\Gamma(\eta)} \sum_{\rho=\theta+k-\eta}^{s-\eta} (s-1-\rho)^{(\eta-1)} f(\rho+\eta-1, y(\rho + \eta - 1)), \quad s \in \mathbb{N}_{\theta+k-\eta}, \tag{6}$$

where

$$y_0(\theta) = \sum_{m=0}^{k-1} \frac{(r-\theta)^m}{\Gamma(m+1)} \Delta^m y(\theta). \tag{7}$$

**Remark 1.** Take $r = n+1, \theta = 0, \rho+\eta-1 = j$ and since $(r-1-\rho)^{(\eta-1)} = \frac{\Gamma(r-\rho)}{\Gamma(r+1-\tau-\eta)}$. Then, for $k=1$, we can obtain the numerical formula of the solution (6) as follows:

$$y(n+1) = y(0) + \frac{1}{\Gamma(\eta)} \sum_{j=0}^{n} \frac{\Gamma(n-j+\eta)}{\Gamma(n-j+1)} f(j, y(j)), \quad 0 < \eta \le 1, \quad n \in \mathbb{N}, \tag{8}$$

where $y(0)$ is the initial condition.

Now, according to Theorem 1 the numerical formula $y_n$ of the DTHNN (4) is expressed as:

$$\begin{cases} y_{n+1}^1 = y_0^1 + \sum_{j=0}^{n} \frac{\Gamma(n-j+\eta)}{\Gamma(\eta)\Gamma(n-j+1)} \left( -y_j^1 + \beta \sin(y_j^1) - \gamma \sin(y_j^2) \right), \\ y_{n+1}^2 = y_0^2 + \sum_{j=0}^{n} \frac{\Gamma(n-j+\eta)}{\Gamma(\eta)\Gamma(n-j+1)} \left( -y_j^2 + \sin(y_j^1) + \beta \sin(y_j^2) \right), \end{cases} \tag{9}$$

where the initial condition $y_0^1 = y_1(0), y_0^2 = y_2(0)$ is given. Let $\beta = 10, \gamma = 7, \eta = 0.99$, and the initial value is $y_0^1 = 0.1, y_0^2 = 0.1$, the phase diagram of system (4) is shown in Fig. 1. Correspondingly, the time evolution of the proposed system (4) is depicted in Fig. 2. One can see from the previous figures that the discrete HNN with fractional order can also show chaotic behaviour. [htp!]

### 2.1. Bifurcation and maximum Lyapunov Exponents analysis

In this section, the fractional order $\eta$ and the system parameters $\gamma, \beta$ are considered as bifurcation parameters, and the dynamical behaviour of the fractional HNN with discrete time is discussed by bifurcation diagrams and maximum Lyapunov exponents (LEs). The maximum LEs is calculated and the Jacobian matrix ($JM_i$) is obtained by employing the Jacobian matrix algorithm of fractional systems [28].

The $JM_i$ matrix of the system (4) is given as:

$$JM_i = \begin{bmatrix} u_i & v_i \\ w_i & z_i \end{bmatrix}, \tag{10}$$

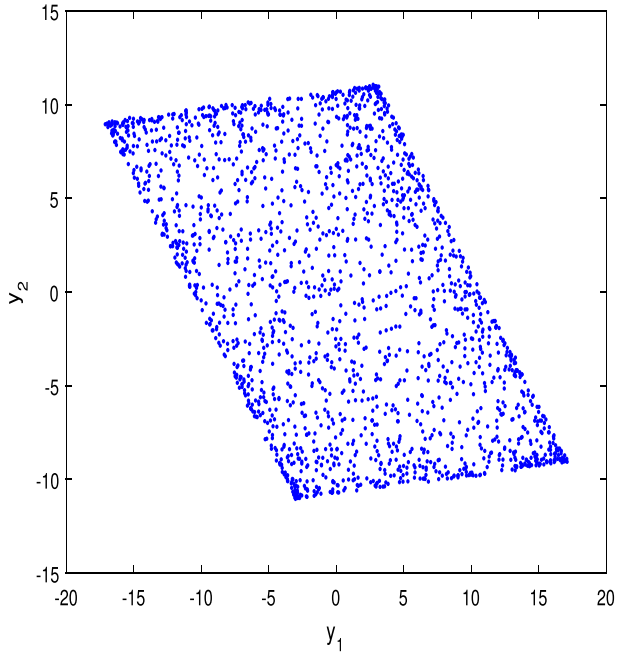


**Fig. 1** The phase portrait of the fractional order discrete HNN (4) for $\eta = 0.99, \beta = 10, \gamma = 7$ and IC $(0.1, 0.1)$.

where

$$\begin{cases} u_i = u_0 + \sum_{j=1}^{i} \frac{\Gamma(i-j+\eta)}{\Gamma(\eta)\Gamma(i-j+1)} \{ u_{j-1}(\beta \cos(y_{j-1}^1) - 1) - \gamma w_{j-1} \cos(y_{j-1}^2) \}, \\ v_i = v_0 + \sum_{j=1}^{i} \frac{\Gamma(i-j+\theta)}{\Gamma(\eta)\Gamma(i-j+1)} \{ v_{j-1}(\beta \cos(y_{j-1}^1) - 1) - \gamma z_{j-1} \cos(y_{j-1}^2) \}, \\ w_i = w_0 + \sum_{j=1}^{i} \frac{\Gamma(i-j+\theta)}{\Gamma(\eta)\Gamma(i-j+1)} \{ w_{j-1}(\beta \cos(y_{j-1}^2) - 1) + u_{j-1} \cos(y_{j-1}^1) \}, \\ z_i = z_0 + \sum_{j=1}^{i} \frac{\Gamma(i-j+\eta)}{\Gamma(\eta)\Gamma(i-j+1)} \{ z_{j-1}(\beta \cos(y_{j-1}^2) - 1) + v_{j-1} \cos(y_{j-1}^1) \}. \end{cases} \tag{11}$$

Then, the LEs have the following formula:

$$LE_k = \lim_{i \to \infty} \frac{1}{i} ln |\lambda_k^{(i)}|, for k = 1, 2, 3. \tag{12}$$

Note that $\lambda_k^{(i)}$ are the eigenvalues of the matrix $JM_i$.

It is known that when the maximum LEs ($\lambda_{max}$) is positive the system is chaotic, whereas when the maximum LEs is negative the system is in periodic state.

The fractional order $\eta$ is always an important indicator to study the stability of the fractional DHNN. Consider the system parameters $\gamma = 7, \beta = 10$, the bifurcation and maximum LEs of the state $y_1$ with respect to $\eta$ are depicted in Fig. 3, in which $\eta$ varies from 0 to 1 by the step size $\Delta\eta = 0.01$. We can observe from the bifurcation diagram represented in Fig. 3(a) that the fractional DHNN (4) is chaotic for all values of the fractional order $\eta$. At the same time, the maximum LEs in Fig. 3(b) agree well with the bifurcation in Fig. 3(a).

In order to analyze the effect of the parameter $\beta$ on the behaviour of the DHNN with fractional order (4), we assign the system parameter to $\gamma = 7$. The bifurcation diagrams of the state $y_1$ and maximum LEs for the 2D fractional DHNN

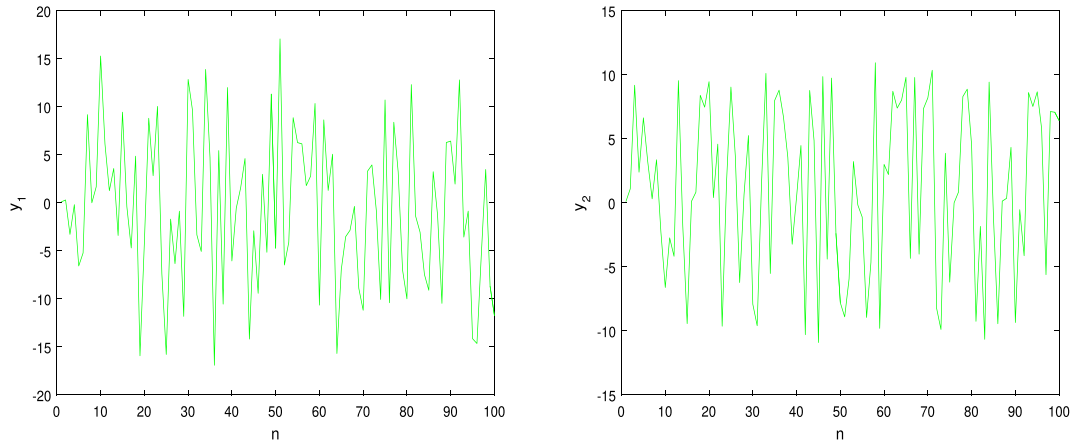


**Fig. 2** The time evolution of the states of the discrete HNN with fractional order (4) for $\beta = 10, \gamma = 7, \eta = 0.99$ and I.C $(0.1, 0.1)$.

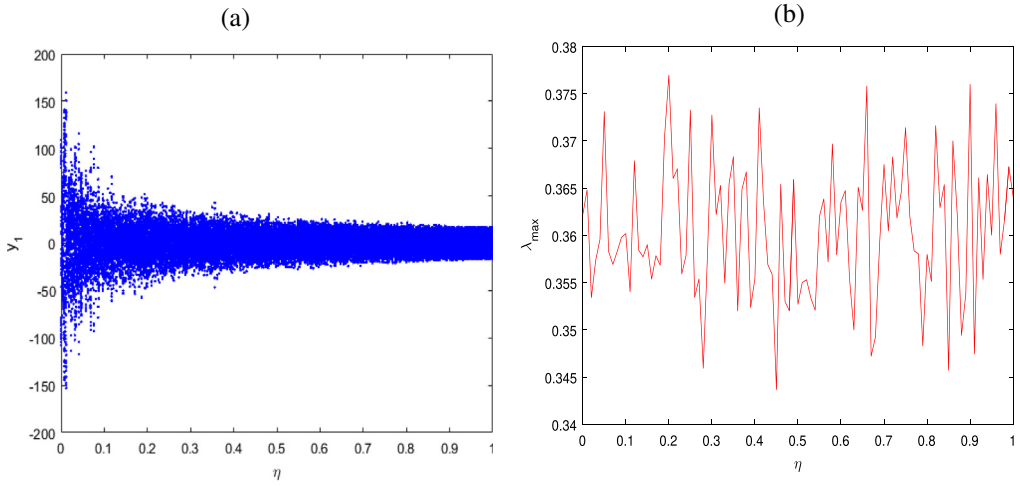


**Fig. 3** Bifurcation and maximum LEs of the fractional HNN with discrete time (4) versus the fractional order $\eta$ with $\gamma = 7, \beta = 10$ and IC $(0.1, 0.1)$.

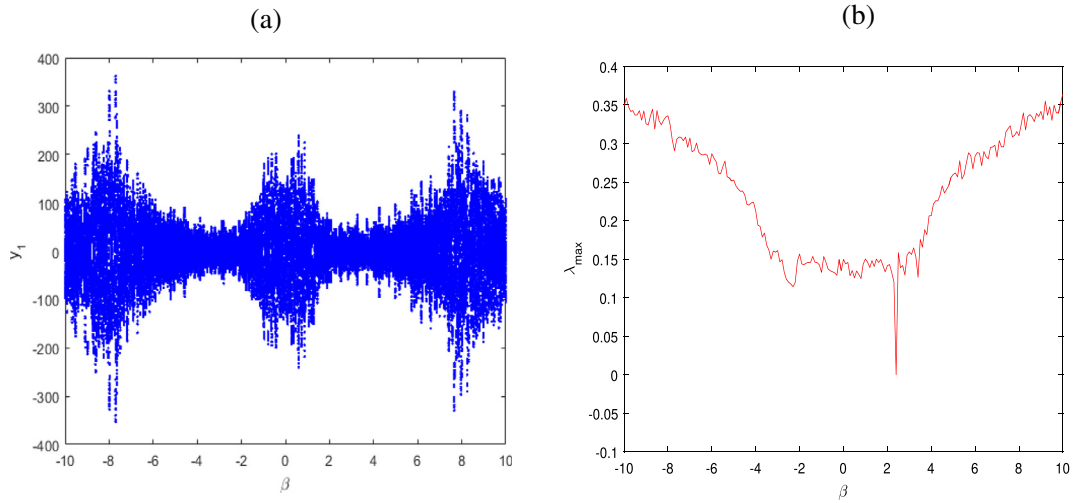


**Fig. 4** Bifurcation and maximum LEs of the DHNN with fractional order (4) versus the system parameter $\beta$ for $\eta = 0.01, \gamma = 7$ and IC $(0.1, 0.1)$.

(4) are numerically simulated as shown in Fig. 4 and Fig. 5 for the initial state $(0.1, 0.1)$, and for two different fractional orders $\eta = 0.01, 0.9$, respectively. We can see from Fig. 4 and Fig. 5 that the fractional DHNN is chaotic for all values of the parameter $\beta \in [-10, 10]$, in the two cases, i.e. when $\eta = 0.01$ and $\eta = 0.9$ where the value of the maximum Lyapunov exponents is greater than zero along the interval $[-10, 10]$ except in the case when $\beta = 2.4$ and $\eta = 0.01$ where the value of the maximum Lyapunov exponents is less than zero which indicate that the system (4) is periodic.

Using the same parameter values and initial condition setting in Fig. 4, the system parameter $\gamma$ is denoted as bifurcation parameter adjusted in the region $[-7, 7]$. The bifurcation plots versus the parameter $\gamma$, with the corresponding maximum LEs are shown in Fig. 6 and Fig. 7, for $\eta = 0.01$ and $\eta = 0.9$, respectively. It can be easily deduced that the DHNN with fractional order (4) is chaotic for all values of the parameter $\gamma$ in the range $[-7, 7]$ and for both fractional order values, which is clearly confirmed by the maximum LEs diagrams.

### 2.2. The approximate entropy of the fractional order DHNN

Now, we describe the complexity of the fractional DHNN (4) using the approximate entropy (ApEn) algorithm [29]. The complexity of a system is the randomness of its chaotic states. The higher values of *ApEn* is, the closer the system sets to a random sequence and, consequently, the more secure the system becomes. For the specific calculating method we consider $N$ points of the state $(y_n^1)_{n=1,\ldots,N}$, and start by defining $n - m + 1$ vectors $Q(k) = [q(k), \ldots, q(k + m - 1)]$, for $k \in [1, n - m + 1]$ where $q(1), q(2), \ldots, q(n)$ is a set of discrete points. Then, the following equation is defined:

$$C_k^m(r) = \frac{L}{n - m + 1}, \tag{13}$$

where $L$ is the number of $Q(k)$ having $d(Q(k), Q(j)) \leqslant r$.

Note that the value of the approximate entropy depends on two important parameters: The embedding dimension $m$ and the similar tolerance $r$, in our work, we set $m = 2$ and $r = 0.2std(q)$ where $std(q)$ is the standard deviation of the data $q$. Theoretically, for $W^m(r) = \frac{1}{n-m-1}\sum_{k=0}^{n-m+1} \log C_k^m(r)$, the *ApEn* is calculated as:

$$ApEn = W^m(r) - W^{m+1}(r). \tag{14}$$

When the system parameter $\beta$ is equal to $10, \gamma = 7$ and the IC is fixed at $(0.1, 0.1)$, the ApEn of the DHNN with fractional order (4) for different values of the fractional order $\eta$ is depicted in Fig. 8. We can see that the complexity of the system increases from 0.1631 to a high level 1.7040 as the value of the fractional order $\eta$ increases in the interval $(0, 1]$, this result agrees well with the results of the bifurcation and maximum LEs diagrams represented in Fig. 3 and confirms that the proposed system (4) has a random behaviour for all $\eta$ in $(0, 1]$.

### 2.3. The $C_0$ complexity of the fractional DHNN

A complexity measure plays important role in analyzing dynamic properties of chaotic systems. There are several methods to measure complexity of time series, including permutation entropy (PE), statistical complexity measure (SCM), sample entropy (SampEn), fuzzy entropy (FuzzyEn), approximate entropy (ApEn), and $C_0$ algorithm. Among them, the $C_0$ complexity is calculated by the fast Fourier transform and through of the new spectra to obtain a new signal. The corresponding complexity value is obtained by the ratio of the area between the difference of the original signal and the new signal and its mean value over the area between the original signal and its mean values. The mathematical foundation of this complexity measure was given in [30]. For a sequence $\{v(0), \ldots, v(M-1)\}$, the algorithm of the $C_0$ complexity is given as follows:

- The discrete Fourier transform of the sequence, $\{v(0), \ldots, v(M-1)\}$, is calculated as:

$$w_M(m) = \sum_{k=0}^{M-1} v(k)\exp^{-2\pi i(km/M)}, \quad m = 0, \ldots, M-1. \tag{15}$$

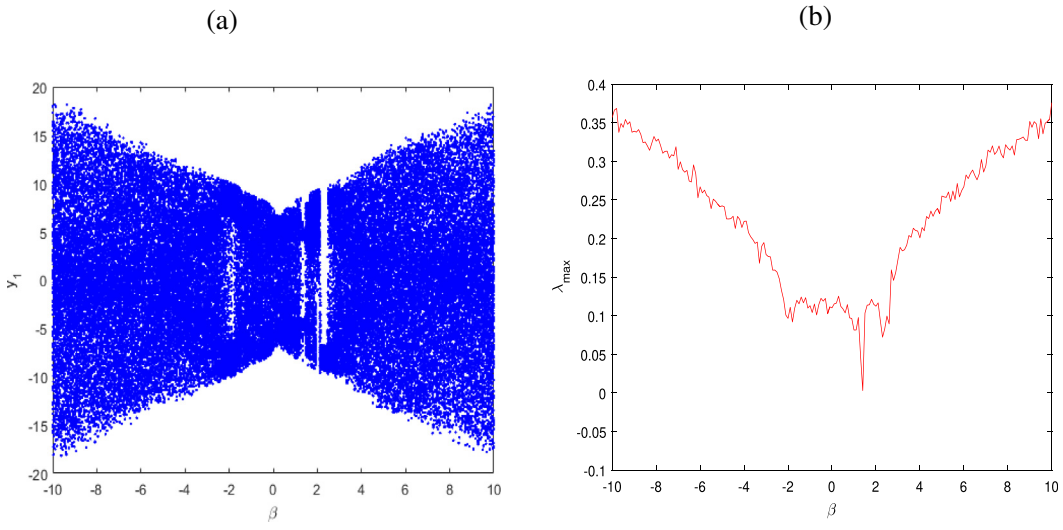


**Fig. 5** Bifurcation and maximum LEs of the DHNN wih fractional order (4) versus the system parameter $\beta$ for $\eta = 0.9, \gamma = 7$ and IC $(0.1, 0.1)$.

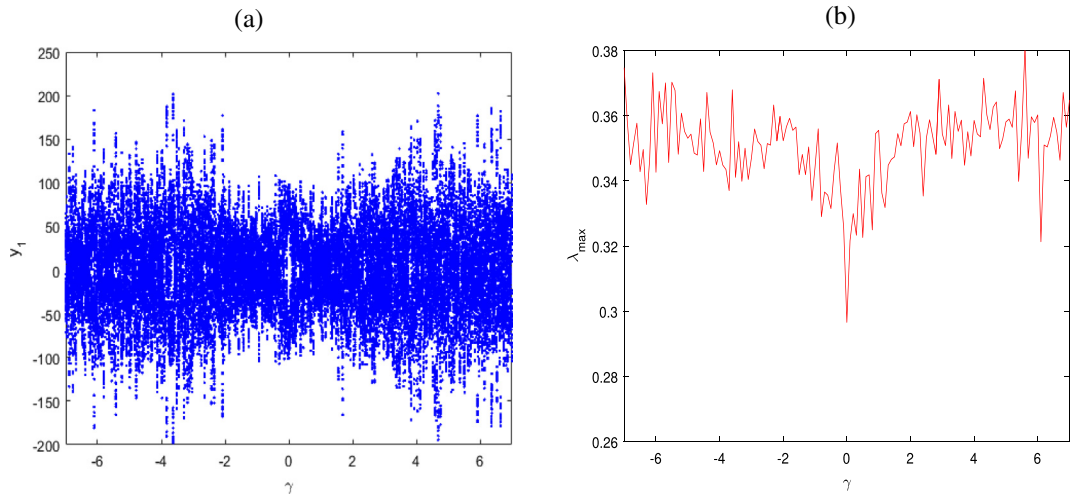


**Fig. 6** Bifurcation and maximum LEs of the DHNN with fractional order (4) versus the parameter $\gamma$ for $\eta = 0.01, \beta = 10$ and IC $(0.1, 0.1)$.

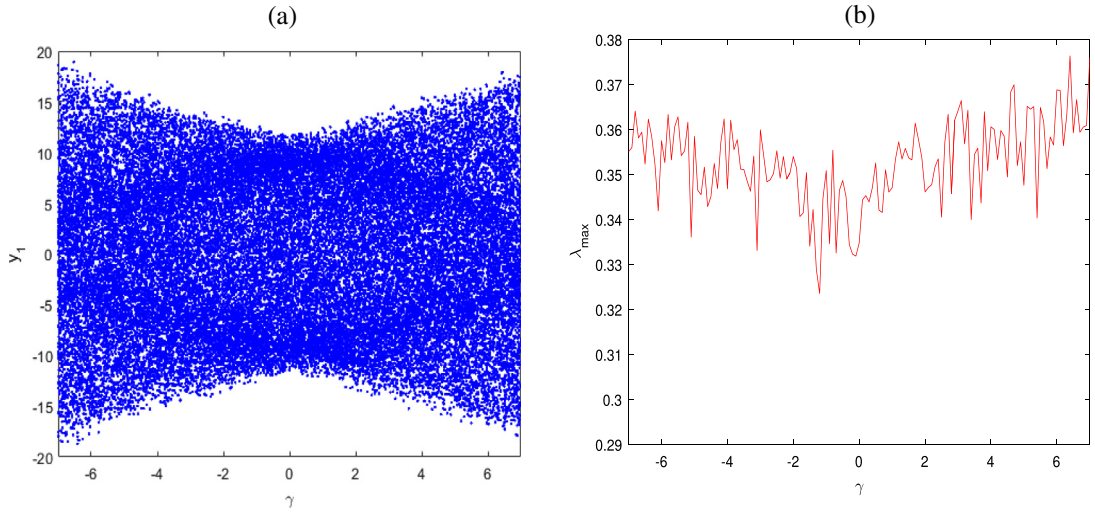


**Fig. 7** Bifurcation and maximum LEs of the DHNN with fractional order (4) versus the parameter $\gamma$ for $\eta = 0.9, \beta = 10$ and IC $(0.1, 0.1)$.

- The mean square value is given as:

$$G_M = \frac{1}{M}\sum_{k=0}^{M-1} |\, w_M(k)|^2. \tag{16}$$

- Import a control parameter $r$. Replace the spectrum component with zero if their square values are plus than $rG_M$, while keep the irregular parts, i.e. the parts which their square are less or equal to $rG_M$, changed as follows

$$\bar{w}_M(k) = \begin{cases} w_M(k) & if \quad |\, w_M(k)|^2 > rG_M, \\ 0 & if \quad |\, w_M(k)|^2 \leqslant rG_M. \end{cases} \tag{17}$$

In the following $r$ is taken as $r = 0.2$.

- The inverse Fourier transform of $\bar{w}_M$ is defined as:

$$\bar{v}(j) = \frac{1}{M}\sum_{k=0}^{M-1} \bar{w}_M(k)\exp^{2\pi i(jk/M)}, j = 0, \ldots, M-1. \tag{18}$$

Finally, we can obtain the formula of the $C_0$ as follows:

$$C_0 = \frac{\sum_{k=0}^{M-1} |\, v(k) - \bar{v}(k)|^2}{\sum_{k=0}^{M-1} |\, v(k)|^2}. \tag{19}$$

Fix $\beta = 10, \gamma = 7$, let $\eta$ varies from 0 to 1, and the initial value of state $(0.1, 0.1)$. The $C_0$ complexity of the fractional DHNN (4) is shown in Fig. 9. We can observe that the complexity of the proposed system (4) is consistent with the change of *ApEn* in Fig. 8 and the change of maximum LEs in Fig. 3.

### 2.4. Control of the DHNN

In this part of research, we present a control scheme to stabilize the states of the fractional DHNN (4). First, we report the following theorem that summarizes the result of [31], which is

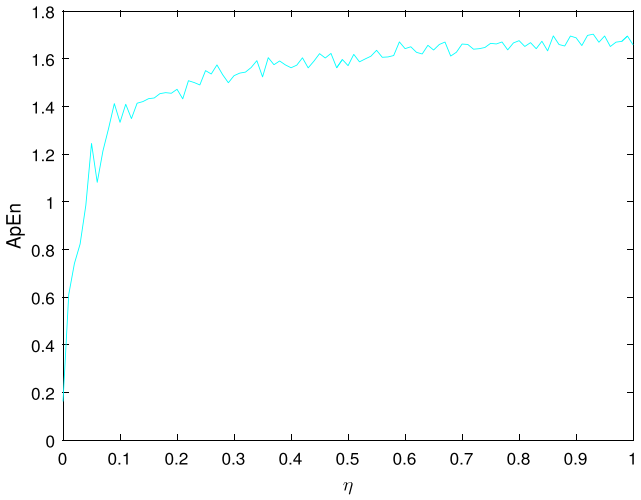


**Fig. 8** The ApEn of the DHNN with fractional order (4) for $\beta = 10, \gamma = 7$ and IC $(0.1, 0.1)$.

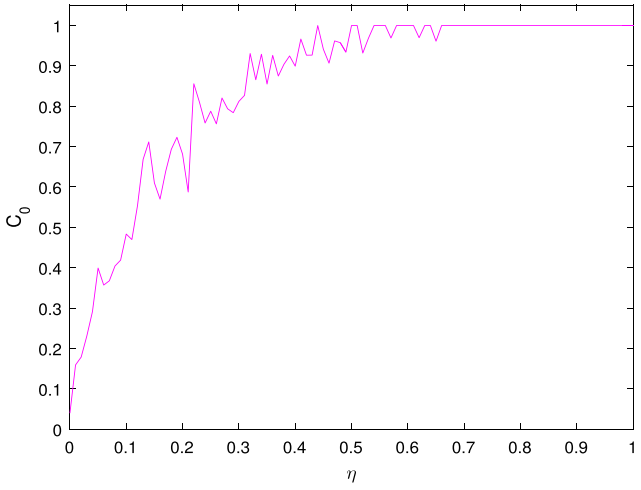


**Fig. 9** The $C_0$ complexity of the DHNN with fractional order (4) for $\beta = 10, \gamma = 7$ and IC $(0.1, 0.1)$.

used to analyze the stabilization of fractional discrete systems. Then, we preform numerical simulation to show the effectiveness of the proposed control technique. Given a vector function $g(t) = (g_1(t), \ldots, g_m(t))^T, 0 < \eta < 1$ and a matrix $B \in \mathbb{R}^{m\times m}$, then the zero equilibrium of the linear discrete system with fractional order

$$ {}^{C}\Delta_{\theta}^{\eta} g(t) = Bg(t + \eta - 1) \tag{20} $$

is asymptotically stable for all $t \in \mathbb{N}_{\theta+1-\eta}$ if the eigenvalues $\lambda$ of the matrix $B$ satisfy

$$ \lambda \in \{w \in \mathbb{C} : \mid w \mid < \left(2\cos\frac{\mid argw \mid -\pi}{2-\eta}\right)^{\eta} and \mid argw \mid > \frac{\eta\pi}{2}\}. \tag{21} $$

Consider the controlled system as follows:

$$ \begin{cases} {}^{C}\Delta^{\eta} y_1(s) = -y_1(s+\eta-1) + \beta\sin(y_1(s+\eta-1)) \\ \qquad\qquad -\gamma\sin(y_2(s+\eta-1)) + u_{y_1}(s+\eta-1), \\ {}^{C}\Delta^{\eta} y_2(s) = -y_2(s+\eta-1) + \sin(y_1(s+\eta-1)) \\ \qquad\qquad +\beta\sin(y_2(s+\eta-1)) + u_{y_2}(s+\eta-1), \end{cases} \tag{22} $$

where $u_{y_1}(s)$ and $u_{y_2}(s)$ represent the adaptive control terms.

The following theorem is stated to obtain our results.

**Theorem 2.** The fractional DHNN (4) is stabilized under the two-dimensional control described as follows:

$$ \begin{cases} u_{y_1}(s) = -\beta\sin(y_1(s)) + \gamma\sin(y_2(s)), \\ u_{y_2}(s) = -\sin(y_1(s)) - \beta\sin(y_2(s)), \end{cases} \tag{23} $$

**Proof 1.** By substituting (23) into (22), we get the following system:

$$ \begin{cases} {}^{C}\Delta^{\eta} y_1(s) = -y_1(s+\eta-1), \\ {}^{C}\Delta^{\eta} y_2(s) = -y_2(s+\eta-1), \end{cases} \tag{24} $$

which can be written as follows:

$$ {}^{C}\Delta^{\eta}(y_1(s), y_2(s))^T = B(y_1(s), y_2(s))^T, \tag{25} $$

where:

$$ B = \begin{bmatrix} -1 & 0 \\ 0 & -1 \end{bmatrix}. \tag{26} $$

The eigenvalues of the matrix $B$ are $\lambda_1 = \lambda_2 = -1$, it is easy to show that the eigenvalues satisfy the condition of Theorem ??, which proves that the zero equilibrium of the controlled system (24) is asymptotically stable, therefore, the states of the controlled system (24) are asymptotically stabilized.

The results of Theorem 2 are illustrated in Fig. 10, Fig. 11 and Fig. 12 with $\beta = 10, \gamma = 7, \eta = 0.5, 0.9$ and IC $(y_1(0), y_2(0)) = (0.1, 0.1)$. Clearly, the controlled system state's converge to zero and the chaotic nature of the system is deleted.

## 3. Variable-order fractional discrete HNN

In this section, we show an alternative representation of the 2D fractional DHNN by using variable order fractional difference operator. The variable order fractional DHNN is obtained by replacing the classical fractional operator with the variable-order Caputo-like difference operator ${}^{C}\Delta_{s}^{\theta(r)}$, i.e:

$$ \begin{cases} {}^{C}\Delta_{s}^{\theta(r)} y_1(r) = -y_1(r+\theta(r)-1) + \beta\sin(y_1(r+\theta(r)-1)) \\ \qquad\qquad -\gamma\sin(y_2(r+\theta(r)-1)), \\ {}^{C}\Delta_{s}^{\theta(r)} y_2(r) = -y_2(r+\theta(r)-1) + \sin(y_1(r+\theta(r)-1)) \\ \qquad\qquad +\beta\sin(y_2(r+\theta(r)-1)). \end{cases} \tag{27} $$

where $r \in \mathbb{N}_{s+1-\theta(r)}, \theta(r) \in (0, 1]$ is the fractional variable order and $s \in \mathbb{R}$ is the stating point.

According to Theorem 1, the numerical formula of the system (27) is given as:

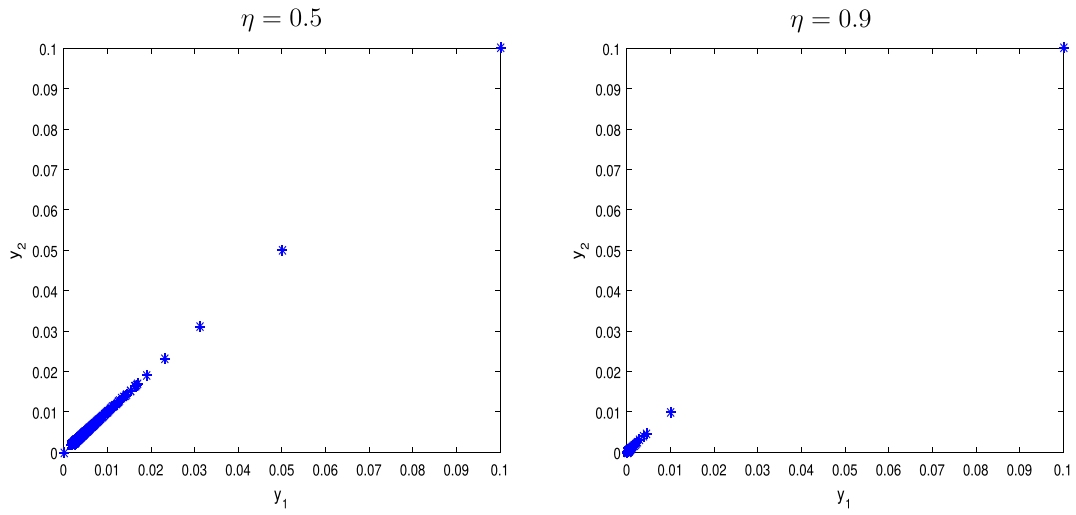


**Fig. 10** Attractors of the controlled system (24) with $\beta = 10, \gamma = 7$ and IC $(0.1, 0.1)$.

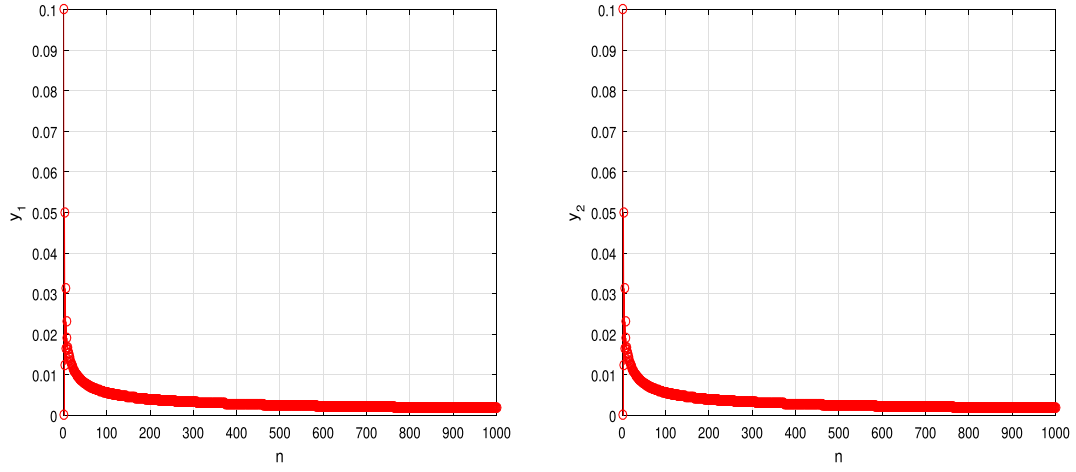


**Fig. 11** The stabilized states of the controlled DHNN with fractional order (24) for $\beta = 10, \gamma = 7$, IC $(0.1, 0.1)$ and fractional order $\eta = 0.5$.

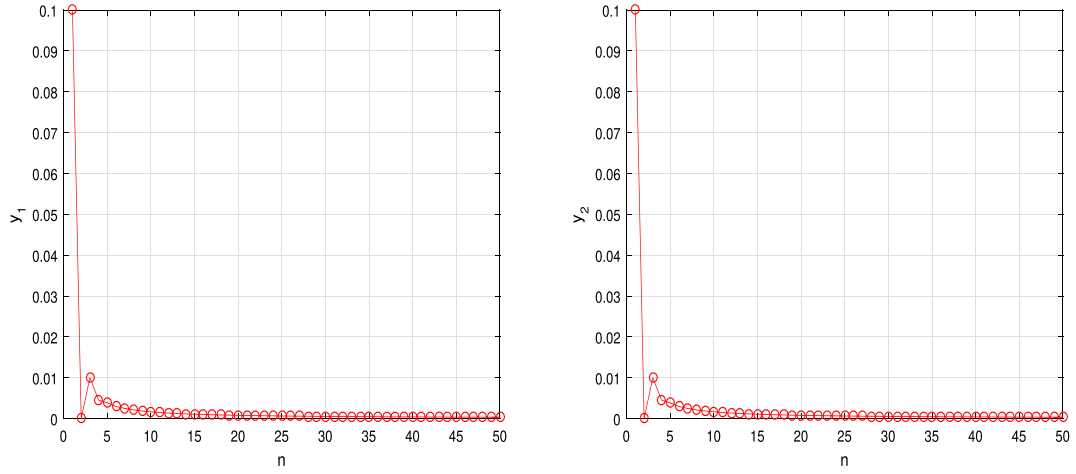


**Fig. 12** The stabilized states of the controlled DHNN with fractional order (24) for $\beta = 10, \gamma = 7$, IC $(0.1, 0.1)$ and fractional order $\eta = 0.9$.

$$\begin{cases} y_{n+1}^1 = y_0^1 + \sum_{j=0}^{n} \frac{\Gamma(n-j+\theta(n))}{\Gamma(\theta(n))\Gamma(n-j+1)} \{-y_j^1 + \beta \sin(y_j^1) \\ \qquad -\gamma \sin(y_j^2)\}, \\ y_{n+1}^2 = y_0^2 + \sum_{j=0}^{n} \frac{\Gamma(n-j+\theta(n))}{\Gamma(\theta(n))\Gamma(n-j+1)} \{-y_j^2 + \sin(y_j^1) \\ \qquad +\beta \sin(y_j^2)\}, \end{cases} \tag{28}$$

with the known initial condition $y_0^1 = y_1(0), y_0^2 = y_2(0)$.

Consider the system parameters $\beta = 10, \gamma = 7$, and the IC $(y_1(0), y_2(0)) = (0.1, 0.1)$. MATLAB numerical simulations are performed and several phase plots are obtained for different fractional variable orders as shown in Fig. 13, from which the chaotic behaviour characterized by a strange attractor is revealed. We can observe that the shape of the attractors of the DHNN with fractional variable order (27) is different from the shape of the attractor of the DHNN with constant fractional order (4) represented in Fig. 1. Therefore, we can say that the choice of the fractional variable order has an influence on the shape of the attractors of the system (27).

Note that all attractors depicted in Fig. 13 for the proposed fractional variable order DHNN prove that the system (27) can exhibit chaotic behaviour.

Since the phase portraits are not definitive to describe the nature of the dynamics of the system, we are going to observe the bifurcation and the maximum Lyapunov exponents plots with respect to the parameters $\beta$ and $\gamma$. When the control parameter is set as $\gamma = 7$ with the initial conditions $(y_1(0), y_2(0)) = (0.1, 0.1)$, the bifurcation diagram of the state $y_1$ and the maximum LEs versus $\beta$ for three different fractional variable orders $\theta(r) = 0.5 + 0.3\cos(0.1r), \theta(r) = 0.7 + 0.2\frac{\exp(-r)}{1+\exp(-r)}$ and $\theta(r) = 0.99 - (0.01/100)r$, are shown in Fig. 14. Complex dynamical phenomena, including period window and chaos can be observed in Fig. 14. It is easy to observe that the shape of the bifurcation diagrams is different for the three proposed fractional variable orders and it is also different from the shape of bifurcation plots represented in Fig. 4 and Fig. 5. These results confirm that the proposed fractional variable order DHNN (27) has chaotic behaviour for the three chosen fractional variable orders where the value of the maximum LEs is greater than zero except in the case when $\theta(r) = 0.99 - (0.01/100)r$ where the value of the maximum LEs is less than zero for $\beta = 1.3$ which indicates that the DHNN (27) is periodic. Now, we fix the parameter $\beta$ at $\beta = 10$, then draw the bifurcation and maximum Lyapunov exponents versus the parameter $\gamma$ for the same fractional variable orders chosen previously as shown in Fig. 15.

Fig. 15 shows that changing the variable order significantly changes the size and state of bifurcation diagram under the same parameters. Basically, the bifurcation diagrams are also different from the diagrams in Fig. 6 and Fig. 7 with constant fractional order. These results prove that the variable fractional order has an effect on the dynamics of the DHNN.

The above numerical simulations demonstrate that even the variable-order fractional DHNN under the variable fractional Caputo operator can describe chaotic behaviour.

## 4. Conclusion and future works

This paper presents a significant contribution to the field of neural networks by proposing a novel discrete Hopfield neural network that incorporates fractional order and variable fractional order using Caputo-like difference form. The variable order is a continuous function that ranges between zero and one. The research demonstrates the emergence of complex dynamics in the system's behaviour by generating phase portraits, bifurcation and maximum Lyapunov exponents plots for varying system parameters, fractional values. The study identifies different types of chaotic attractors within the conceived network and observes a higher level of complexity in comparison to a network with constant fractional order. Moreover, the research highlights the importance of selecting the appropriate fractional order value in determining the dynamics of the discrete Hopfield neural network is validated through stability theory and numerical simulations demonstrating the convergence of states to the zero solution. The research suggests that control offers additional flexibility and may enable the development of novel control strategies in related fields.

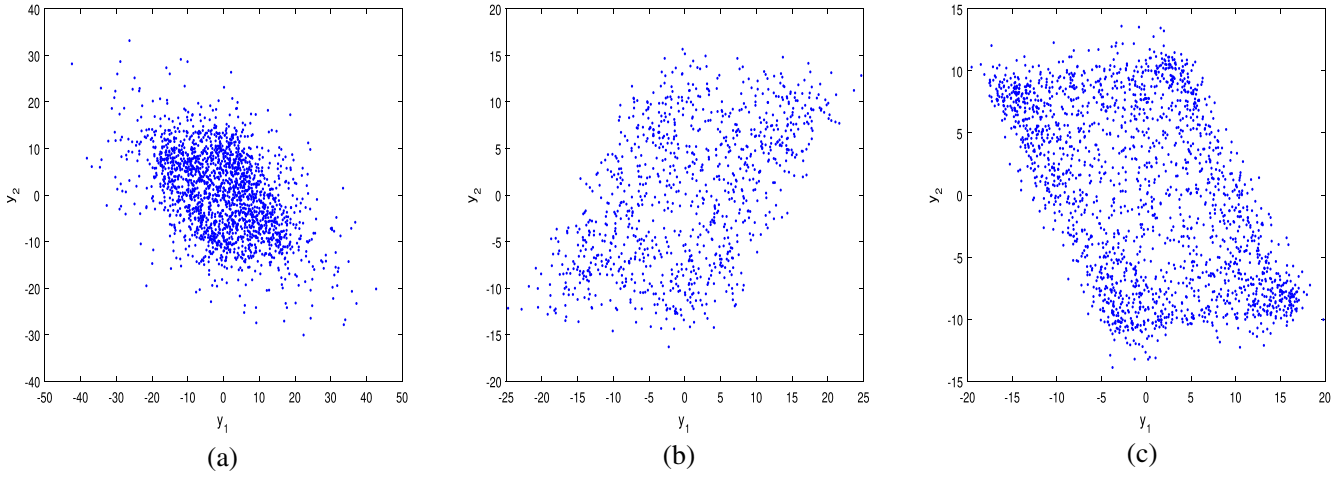


**Fig. 13** The phase portraits of the variable fractional order DHNN (27) for different fractional variable orders $\theta(r)$ with $\beta = 10, \gamma = 7$ and IC $(0.1, 0.1)$ : $(a)$ $\theta(r) = 0.5 + 0.3\cos(0.1r)$, $(b)$ $\theta(r) = 0.7 + 0.2\frac{\exp(-r)}{1+\exp(-r)}$, $(c)$ $\theta(r) = 0.99 - (0.01/100)r$.

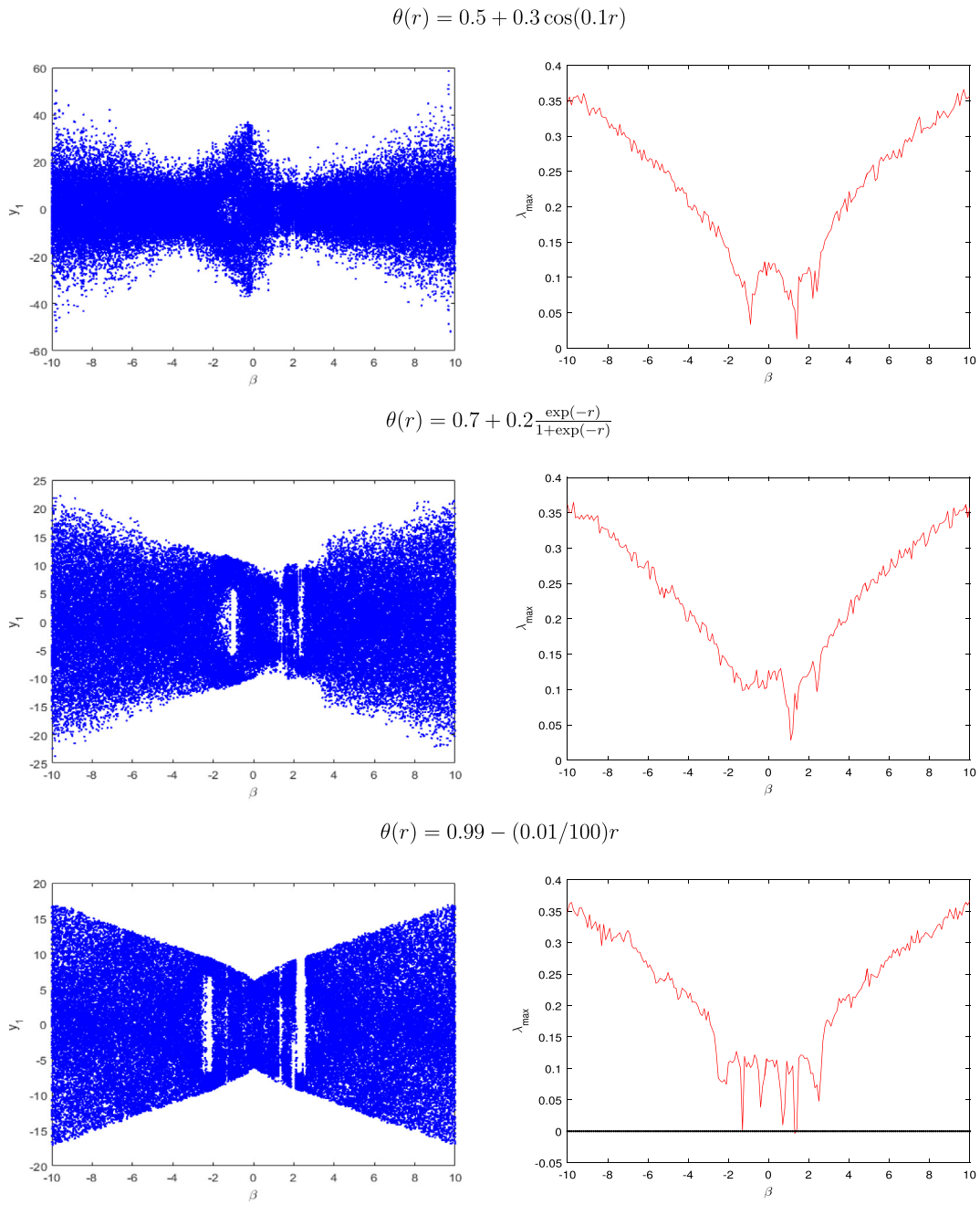


**Fig. 14** Bifurcation and maximum LEs of the variable fractional order DHNN (27) versus the parameter $\beta$ for different fractional variable orders with $\gamma = 7$ and I.C $(0.1, 0.1)$.

$$\theta(r) = 0.5 + 0.3\cos(0.1r)$$

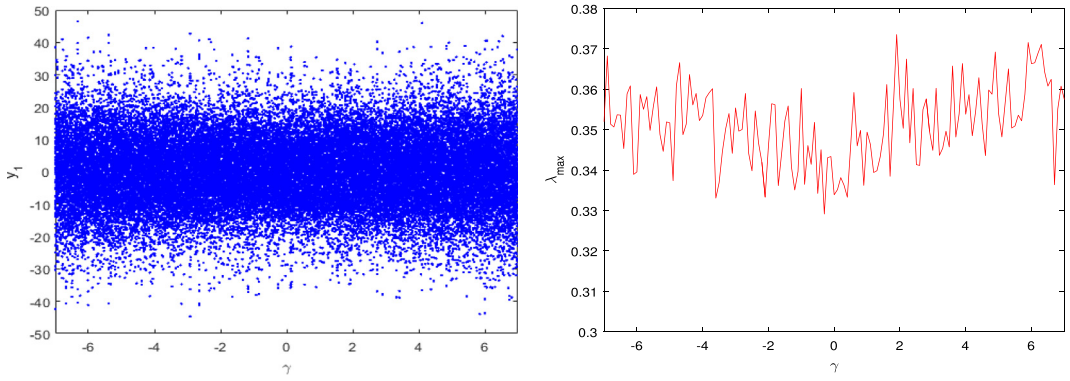


$$\theta(r) = 0.7 + 0.2\frac{\exp(-r)}{1+\exp(-r)}$$

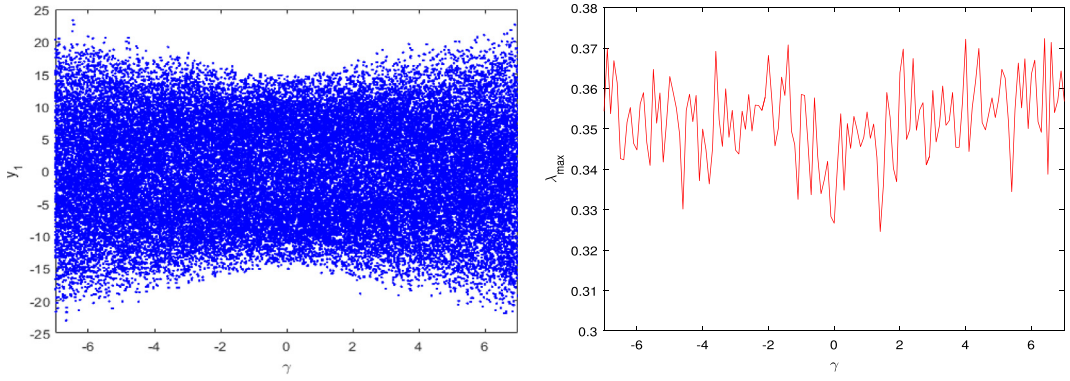


$$\theta(r) = 0.99 - (0.01/100)r$$

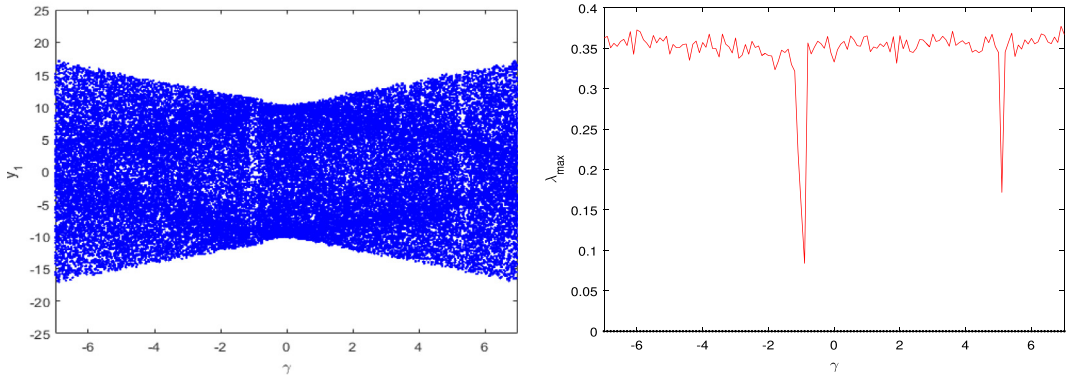


**Fig. 15** Bifurcation and maximum LEs diagrams of the variable order fractional DHNN (27) versus the parameter $\gamma$ for different fractional variable orders with $\beta = 10$ and IC (0.1,0.1).

Finally, due to the rich complex behaviour exhibited by the proposed system, we conclude that the concept of fractional variable-order is a powerful tool for modelling fractional discrete neural network of Hopfield type.

## Declaration of Competing Interest

The authors declare that they have no known competing financial interests or personal relationships that could have appeared to influence the work reported in this paper.

## References

[1] K.M. Owolabi, A. Atangana, Chaotic behaviour in system of noninteger-order ordinary differential equations, Chaos, soliton & fractal. 115 (2018) 362–370.
[2] K.M. Owolabi, Modelling and simulation of a dynamical system with the Atan- gana–Baleanu fractional derivative, Eur Phys J Plus. 133 (2018) 1–13.
[3] K.M. Owolabi, J.F. Gómez-Aguilar, Numerical simulations of multilingual competition dynamics with nonlocal derivative, Chaos, soliton & fracta. 117 (2018) 175–182.

[4] I.M. Batiha, S. Momani, A. Ouannas, Z. Momani, S.B. Hadid, Fractional-order COVID-19 pandemic outbreak: modeling and stability analysis, Int. J. Biomath. 15 (2022) 2150090.
[5] N. Djenina, A. Ouannas, T.E. Oussaeif, G. Grassi, I.M. Batiha, S. Momani, On the stability of incommensurate h-Nabla fractional-order difference systems, Fractal Fract. 6 (2022) 153.
[6] M.T. Shatnawi, N. Djenina, A. Ouannas, I.M. Batiha, G. Grassi, Novel convenient conditions for the stability of nonlinear incommensurate fractional-order difference systems, Alex. Eng. J. 61 (2022) 1655–1663.
[7] J. Ni, L. Liu, C. Liu, X. Hu, Fractional order fixed-time nonsingular terminal sliding mode synchronization and control of fractional order chaotic systems, Nonlinear Dyn. 89 (2017) 2065–2083.
[8] G. Li, X. Zhang, H. Yang, Complexity analysis and synchronization control of fractional-order Jafari-Sprott chaotic system, IEEE Access. 8 (2020) 53360–53373.
[9] J. Fleck, Development and establishment in artificial intelligence, Ce Question of Artificial Intelligence 16 (2018) 106–164.
[10] S. Hayman, IJCNN'99. International Joint Conference on Neural Networks. Proceedings (Cat. No. 99CH36339), IEEE. 6(1999), 4438–4439.
[11] S. Zhang, Y. Yu, H. Wang, Mittag-Leffler stability of fractional-order Hopfield neural networks, Nonlinear Anal.-Hybri. 16 (2014) 104–121.
[12] A. Gasri, A. Ouannas, A.A. Khennaoui, G. Grassi, T.E. Oussaeif, V.T. Pham, Chaotic fractional discrete neural networks based on the Caputo h-difference operator: stabilization and linear control laws for synchronization, Eur. Phys. J. Spec. Top. 231 (2022) 1–15.
[13] M. Mellah, A. Ouannas, A.A. Khennaoui, G. Grassi, Fractional discrete neural networks with different dimensions: Coexistence of complete synchronization, antiphase synchronization and full state hybrid projective synchronization, Nonlinear Dyn. 21 (2021) 410–419.
[14] I. Batiha, A. Ouannas, J.A. Emwas, A stabilization approach for a novel chaotic fractional-order discrete neural network, Math. Comput. Sci. 11 (2021) 5514–5524.
[15] A. Hioual, T.E. Oussaeif, A. Ouannas, G. Grassi, I.M. Batiha, S. Momani, New results for the stability of fractional-order discrete-time neural networks, Alex. Eng. J. 61 (2022) 10359–10369.
[16] S. Zhou, H. Li, Z. Zhu, Chaos control and synchronization in a fractional neuron network system, Chaos, Solitons Fractals. 36 (2008) 973–984.
[17] N. Debbouche, A. ounnas, I. Batiha, M. Iqbal, et al, Chaotic behavior analysis of a new incommensurate fractional-order hopfield neural network system, Complexity 2021 (2021) 1–11.
[18] A. Hioual, A. Ouannas, T. Oussaeif, G. Grassi, I.M. Batiha, S. Momani, On variable-order fractional discrete neural networks: Solvability and stability, Fractal. Fract. 6 (2022) 119.
[19] A. Hioual, A. Ouannas, On fractional variable-order neural networks with time-varying external inputs, I.J.M. 1(2022) 52–65.
[20] R.C. Karoun, A. Ouannas, M.A. Horani, G. Grassi, The effect of Caputo fractional variable difference operator on a discrete-time Hopfield neural network with non-commensurate order, Fractal. Fract. 6 (2022) 575.
[21] L.L. Huang, J.H. Park, G.C. Wud, Z.W. Moa, Variable-order fractional discrete-time recurrent neural networks, J. Comput. Appl. Math. 370 (2020) 112633.
[22] J.J. Hopfield, Neurons with graded response have collective computational properties like those of two-state neurons, PNAS. 81 (1984) (1984) 3088–3092.
[23] I.M. Batiha, R.B. Albadarneh, S. Momani, I.H. Jebril, Dynamics analysis of fractional-order Hopfield neural networks, Int. J. Biomath. 13 (2020) 2050083.
[24] N. Debbouche, A. Ouannas, I.M. Batiha, G. Grassi, M.K.A. Kaabar, Chaotic behavior analysis of a new incommensurate fractional-order Hopfield neural network system, J. Complex. 2021 (2021) 1–11.
[25] Y. Xi, Y. Yu, S. Zhang, X. Hai, Finite-time robust control of uncertain fractional-order Hopfield neural networks via sliding mode control, Chin. Phys. B. 27 (2018) 010202.
[26] T. Abdeljawad, On Riemann and Caputo fractional differences, Comput. Math. Appl. 62 (2011) 1602–1611.
[27] F. Chen, L. Xiannan, Z. Yong, Existence results for nonlinear fractional difference equation, Adv Differ Equ. 2011 (2011) 1–12.
[28] G.C. Wu, D. Baleanu, Jacobian matrix algorithm for Lyapunov exponents of the discrete fractional maps, Commun. Nonlinear Sci. Numer. Simul. 22 (2015) 95–100.
[29] S.M. Pincus, Approximate entropy as a measure of system complexity, Proc. Natl. Acad. Sci. U.S.A. 88 (1991), 2297–2230.
[30] J. Ran, Discrete chaos in a novel two-dimensional fractional chaotic map, Adv. Differ. Eq. 2018 (2018) 1–12.
[31] J. Čermák, I. Győri, L. Nechvátal, On explicit stability conditions for a linear fractional difference system, Fract Calc Appl Anal. 18 (2015) 651–672.